Direct evidence for a half-metallic ferromagnet

J.-H. Park*, E. Vescovo*, H.-J. Kim*, C. Kwon†‡, R. Ramesh† & T. Venkatesan†

** NSLS Brookhaven National Laboratory, Upton, New York 11973-5000, USA*
† Center for Superconductivity Research, Department of Physics, University of Maryland, College Park, Maryland 20742, USA

Half-metallic materials are characterized by the coexistence of metallic behaviour for one electron spin and insulating behaviour for the other. Thus, the electronic density of states is completely spin polarized at the Fermi level, and the conductivity is dominated by these metallic single-spin charge carriers. This exotic physical property could have a significant effect on technological applications related to magnetism and spin electronics. Some ferromagnetic systems, such as Heusler compounds[1] and chromium dioxide[2], have been predicted theoretically to be half-metallic. However, a half-metallic system has not been demonstrated directly and the predictions are still in doubt[3,4]. Here we report spin-resolved photoemission measurements of a ferromagnetic manganese perovskite, $La_{0.7}Sr_{0.3}MnO_3$, which directly manifest the half-metallic nature well below the Curie temperature. For the majority spin, the photoemission spectrum clearly shows a metallic Fermi cut-off, whereas for the minority spin, it shows an insulating gap with disappearance of spectral weight at ~0.6 eV binding energy.

Half-metallic ferromagnets were introduced by de Groot *et al.*[1], who predicted a metallic character for majority-spin electrons but an insulating character—that is, the Fermi energy (E_F) falls in a gap—for minority-spin electrons, in the spin-polarized band-structure calculation for a Mn-based Heusler alloy NiMnSb[2]. The half-metallic ferromagnet has 100% spin polarization for the conduction electrons, and thus it offers potential technological applications such as a single-spin electron source, and high-efficiency magnetic sensors. The half-metallic feature has also been predicted[2] for a prototypical ferromagnetic oxide CrO_2. However, spin-resolved photoemission studies have not confirmed these predictions. In the case of NiMnSb, only ~50% spin polarization was reported for the conduction electrons[3]. For CrO_2, ~100% spin polarization was observed at ~2 eV binding energy rather than at E_F, where almost no spectral weight appears for both spin electrons, and even the metallic character was questioned[4]. The photoemission measurements are rather surface sensitive, and it is known that it is quite difficult to obtain proper stoichiometry at the surface of both these systems. Thus, it has been often suggested that the results might be influenced by surface segregation effects[3,5].

Doped manganese perovskites with a formula $Ln_{1-x}A_xMnO_3$ (where Ln is a trivalent rare-earth element and A is a divalent alkaline-earth element) have attracted considerable interest, particularly with reference to their potential technological applications. On cooling, these compounds show a large decrease in resistivity associated with a paramagnetic to ferromagnetic transition[6,7]. This transition is known to give rise to a large negative magnetoresistance, the so-called colossal magnetoresistance (CMR)[8,9], near the Curie temperature, T_C. The ferromagnetic ground state has been explained by the double-exchange model[10]. However, a model considering primarily the spin-dependent electron hopping mechanism turns out not to be able to explain the insulator-like high resistivity above T_C. Recent theoretical and experimental studies indicate that small polaron effects (including the Jahn–Teller distortion), as well as the double-exchange model, are required for understanding of the transition and the transport measurements[11–13].

The doped manganese perovskite is mixed-valent with Mn^{3+} ($3d^4$) and Mn^{4+} ($3d^3$). For the octahedral site symmetry of the MnO_6 complex, the configuration becomes $t_{2g}^3e_g^1$ (^5E) for Mn^{3+} and t_{2g}^3 ($^4A_2$) for Mn^{4+}. In the double-exchange mechanism, the e_g electrons are considered as mobile charge carriers interacting with the localized Mn^{4+} ($S = 3/2$) spins. The carrier hopping avoids the strong on-site Hund rule exchange energy J_{ex} when the Mn spins are aligned ferromagnetically. J_{ex} (~2.5 eV) is much larger than the e_g band width (~1 eV). Thus the conclusion electrons are expected to be highly spin polarized, and the possibility of 100% spin polarization (that is, a half-metallic state) has been discussed[14–16]. However, a band-structure calculation[17] of $La_{2/3}Ca_{1/3}MnO_3$ predicted ~36% spin polarization at E_F, and previous spin-resolved tunnelling measurements reported 54% (ref. 18) and 81% (ref. 19) polarization for the conduction electrons of $La_{0.67}Sr_{0.33}MnO_3$ tunnel junctions.

We grew a 1,900-Å-thick $La_{0.7}Sr_{0.3}MnO_3$ epitaxial thin film on a (001) $SrTiO_3$ single-crystal substrate by conventional pulse laser deposition. The surface roughness of the sample is expected to be ~20 Å, and the T_C was determined to be ~350 K. The details of sample growth and characterization are described elsewhere[20]. The measurements were performed at the new U5UA undulator beamline at the National Synchrotron Light Source (NSLS) in the Brookhaven National Laboratory[21]. During the measurements, the base pressure was kept better than 1×10^{-10} torr. The sample was introduced into a vacuum, and the surface was cleaned *in situ* in a sequence of annealing processes, which will be presented in detail elsewhere. The T_C at the surface turns out to be nearly identical to that of the film, indicating that the deviation of the oxygen stoichiometry at the surface is negligible. The photoelectrons were collected by an electron analyser with ±2° angular resolution. However, the spectrum does not display any noticeable angular dependence, indicating that the momentum (**k**) resolution in reciprocal space, which requires a well defined surface normal, is completely obscured owing to the rough surface. Thus, the results obtained can be considered as angle-integrated.

Successful achievement of a clean surface was confirmed in our measurements of temperature-dependent high-resolution photoemission. Figure 1 shows the spectra near E_F measured at two different temperatures, $T = 40$ K ($\ll T_C$) and $T = 380$ K ($> T_C$). The electronic change through the ferromagnetic transition is clearly visible: at $T = 380$ K, the spectrum shows negligible spectral weight at E_F, whereas at $T = 40$ K it clearly shows the metallic Fermi cut-off. In detailed temperature-dependence studies, we also

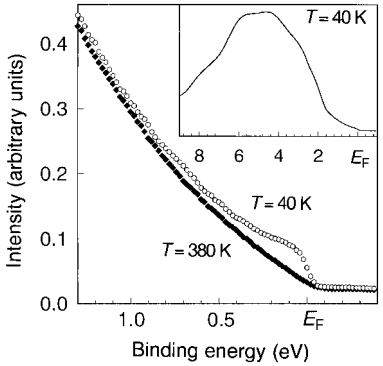

Figure 1 High-resolution photoemission spectra of a thin film of $La_{0.7}Sr_{0.3}MnO_3$, very near the Fermi energy (E_F). The T_C of the sample was ~350 K, measurements were taken at $T = 40$ K ($\ll T_C$; **a**) and at $T = 380$ K ($> T_C$; **b**). The photon energy and the experimental resolution were set at $h\nu = 40$ eV, and $\Delta E = 0.1$ eV, respectively. The inset shows the wide-scan valence band spectrum at $T = 40$ K.

‡ Present address: Superconductivity Technology Center, Los Alamos National Laboratory, Los Alamos, NM 87545, USA.

observed an increase of the spectral weight at E_F with cooling below T_C. This temperature dependency is now well known to be one of the peculiar characteristics of the doped manganese perovskites[12,22]. The wide-range spectrum shown in Fig. 1 inset is also very similar to that reported for bulk polycrystalline $La_{1-x}Sr_xMnO_3$ samples[22]. The electronic state above T_C of $La_{1-x}Sr_xMnO_3$ ($0.17 < x < 0.5$) is not yet well characterized; the temperature dependence of the resistivity of such compounds becomes more metallic-like with increasing of the Sr concentration x, in spite of their high resistance above T_C (ref. 7). However, the spectroscopic measurements show only negligible spectral weight at E_F without the metallic feature, and the high-temperature state has been suggested to be a pseudogap state[12,22,23].

The electrical and magnetic properties of $La_{1-x}Sr_xMnO_3$ thin films are known to be nearly identical to those of the bulk samples[7,20,24], but their magnetic domain behaviour turns out to be completely different from that of the bulk, possibly because of surface stress and finite-size effects. The bulk crystals typically required fields of several teslas to saturate the magnetization and yielded very little remanent magnetization. However, as shown in Fig. 2a, inset, the $La_{0.7}Sr_{0.3}MnO_3$ thin-film sample shows a single-domain-type magnetic hysteresis, that is ~100% remanent magnetization and low coercive field (~100 Oe at 40 K). This single-domain-type behaviour is crucial in opening up the possibility of spin-resolved photoemission studies.

Figure 2 shows valence band spin-resolved photoemission spectra near E_F of the $La_{0.7}Sr_{0.3}MnO_3$ thin film that we measured at

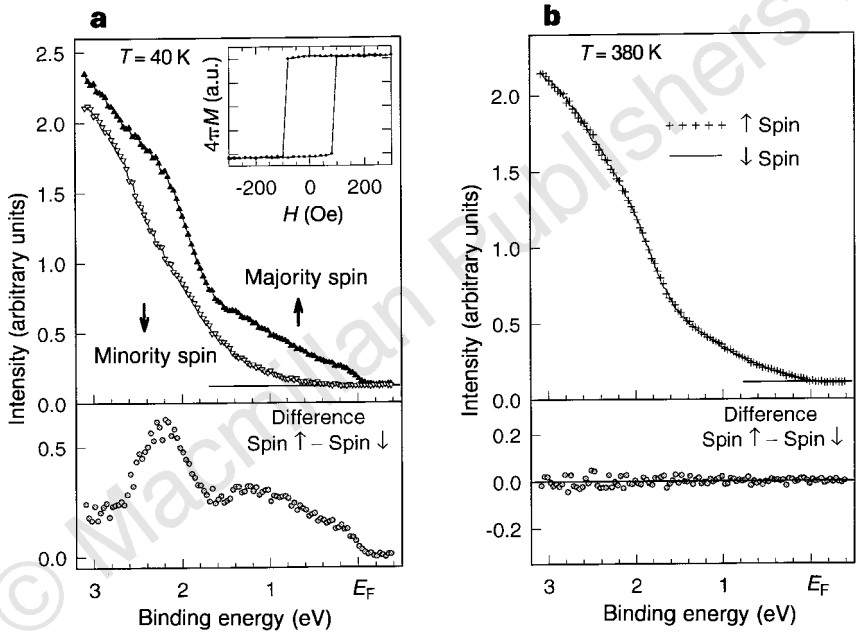

Figure 2 Spin-resolved photoemission spectra of a thin films of $La_{0.7}Sr_{0.3}MnO_3$ (as in Fig. 1), near the Fermi energy (E_F). Measurements were taken at $T = 40$ K ($\ll T_C$; **a**) and at $T = 380$ K ($> T_C$; **b**). The photon energy and the experimental resolution were set at $h\nu = 40$ eV, and $\Delta E = 0.2$ eV, respectively. A magnetic pulse coil with ~200 Oe magnetic field was used for magnetization of the sample. The majority (↑) and minority (↓) spins represent the spin directions respectively parallel and anti-parallel to the magnetization direction. The bottom panels of **a** and **b** show the difference spectra between the majority-spin and the minority-spin spectra. The inset in **a** shows the magnetization (M) versus applied magnetic field (H) hysteresis loop, which was obtained by monitoring Mn L_2-edge absorption intensity for circularly polarized incident light at the NSLS U4B beamline.

Figure 3 Schematic energy diagrams and the Mn 3*d* spin alignments of the doped manganese perovskites at $T \ll T_C$ and at $T > T_C$. J_{ex} is the Hund rule exchange energy, and $E_{gap}\downarrow$ denotes the insulating bandgap of the minority-spin states.

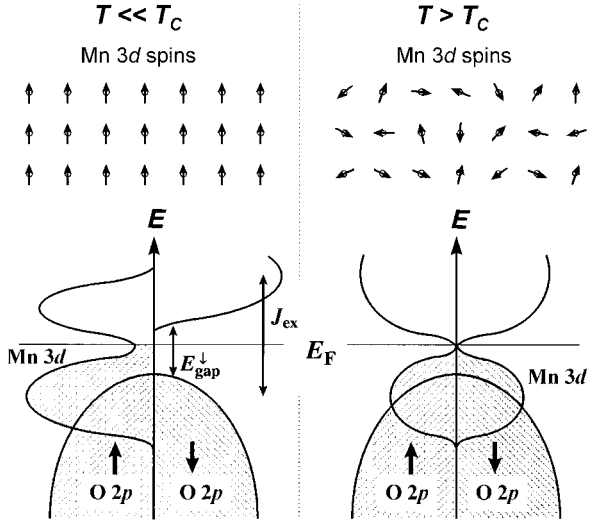

$T = 40$ K (Fig. 2a) and $T = 380$ K (Fig. 2b). At $T = 40$ K ($\ll T_C$), all the Mn 3*d* electron spins are aligned ferromagnetically. Indeed, the spectra in Fig.2a show considerable difference for the majority (↑) and minority (↓) spins. The most striking observation is the half-metallic feature. The spectrum for the majority spin extends up to E_F and shows the metallic Fermi cut-off, while that for the minority spin decreases rapidly at ~1 eV binding energy and the spectral weight disappears very near E_F, reflecting the insulating gap. In the region of 0 to ~0.4 eV binding energy, the minority-spin states only show spectral noise which is also present above E_F, and the spin polarization is found to be 100 ± 5%. Considering the spectral broadening due to the finite experimental resolution, we estimate the half-gap on the occupied state (photoemission) side of the minority-spin states to be 0.6 ± 0.2 eV.

The minority-spin states still show large spectral weight in the higher-binding-energy region owing to the O 2*p* states, which are fully occupied for both spins. The Mn 3*d* state spectrum can be obtained by subtracting the minority-spin spectrum from the majority-spin spectrum. The difference spectrum presented in the bottom panel of Fig. 2a shows the metallic Fermi cut-off at E_F and two peak features around 1.2 eV and 2.2 eV binding energies, which can be interpreted as the e_g and t_{2g} electron removal states, respectively[12]. A similar line shape was previously observed in Mn L_3-edge on-resonant photoemission spectra of bulk $La_{0.67}Ca_{0.33}MnO_3$ and $La_{0.7}Pb_{0.3}MnO_3$, in which the Mn 3*d* states are enhanced exclusively[12].

On heating through T_C, the Mn 3*d* spins become disordered, and the spin anisotropy disappears. The spin-resolved photoemission spectra above T_C confirm the disappearance of the spin anisotropy. The spectra in Fig. 2b, which were measured at $T = 380$ K ($> T_C$), show no difference for the two different spins, and the spectral weight disappears at E_F for both spins, showing the pseudogap feature. The difference spectrum of the up (↑) spin and down (↓) spin spectra, presented in the bottom panel of Fig. 2b, exhibits only experimental noise.

Our spin-resolved photoemission studies of $La_{0.7}Sr_{0.3}MnO_3$ show (1) the half-metal feature well below T_C and (2) the occurrence of the metal to pseudogap state transition accompanied by loss of the ferromagnetic order on heating through T_C. These results are summarized schematically in Fig. 3. At $T \ll T_C$, the Mn 3*d* electron spins are aligned ferromagnetically owing to the ferromagnetic double-exchange interaction. Thus, the Mn 3*d* states, which extend up to E_F, have only the majority spin. However, the O 2*p* states, which have both majority and minority spins, only reach to ~0.6 eV below E_F. Therefore, the majority-spin states show the metallic feature with charge carriers from Mn 3*d* states, whereas the minority-spin states exhibit an insulating gap between the occupied O 2*p* states and the unoccupied Mn 3*d* minority-spin states. At $T > T_C$, the Mn 3*d* spins become disordered and the spin anisotropy disappears. According to the double-exchange mechanism, the loss of ferromagnetic order reduces the electron hopping energy and the density of states at E_F almost disappears; this results from the competition of the electron hopping energy and the small polaron effects, including the Jahn–Teller distortion[11–13]. □

Received 18 June 1997; accepted 27 January 1998.

1. de Groot, R. A., Muller, F. M., van Engen, P. G. & Buschow, K. H. J. New class of materials: half-metallic ferromagnets. *Phys. Rev. Lett.* **50,** 2024–2027 (1983).
2. Schwarz, K. CrO_2 predicted as a half-metallic ferromagnet. *J. Phys. F* **16,** L211–L215 (1986).
3. Bona, G. L., Meier, F., Taborelli, M., Bucher, E. & Schmidt, P. H. Spin polarized photoemission from NiMnSb. *Solid State Commun.* **56,** 391–394 (1985).
4. Kämper, K. P., Schmitt, W., Güntherodt, G., Gambin, R. J. & Ruf, R. CrO_2—a new half-metallic ferromagnet? *Phys. Rev. Lett.* **59,** 2788–2791 (1988).
5. Hanssen, K. E. H. M., Mijnarends, P. E., Rabou, L. P. L. M. & Buschow, K. H. J. Positron-annihilation study of the half-metallic ferromagnet NiMnSb: experiment. *Phys. Rev. B* **42,** 1533–1540 (1990).
6. Jonker, G. H. & van Santen, J. H. Ferromagnetic compounds of manganese with perovskite structure. *Physica* **16,** 337–349 (1950).
7. Tokura, Y. *et al.* Giant mangetotransport phenomena in filling-controlled Kondo lattice system: $La_{1-x}Sr_xMnO_3$. *J. Phys. Soc. Jpn* **63,** 3931–3935 (1994).
8. von Helmholt, R., Wecker, J., Holszapfel, B., Schultz, L. & Samwer, K. Giant negative magnetoresistance in perovskitelike $La_{2/3}Ba_{1/3}MnO_x$ ferromagnetic films. *Phys. Rev. Lett.* **71,** 2331–2334 (1993).
9. Jin, S. *et al.* Thousandfold change in resistivity in magnetoresistive La-Ca-Mn-O films. *Science* **264,** 413–415 (1994).
10. Zener, C. Interaction between the d-shells in the transition metals. II. Ferromagnetic compounds of manganese with perovskite structure. *Phys. Rev.* **82,** 403–405 (1951).
11. Millis, A. J., Shraiman, B. I. & Mueller, R. Dynamic Jahn–Teller effect and colossal magnetoresistance in $La_{1-x}Sr_xMnO_3$. *Phys. Rev. Lett.* **77,** 175–178 (1996).
12. Park, J.-H. *et al.* Electronic aspects of the ferromagnetic transition in manganese perovskites. *Phys. Rev. Lett.* **76,** 4215–4218 (1996).
13. de Teresa, J. M. *et al.* Evidence for magnetic polarons in the magnetoresistive perovskites. *Nature* **386,** 256–258 (1997).
14. Okimoto, Y. *et al.* Anomalous variation of optical spectra with spin polarization in double exchange ferromagnet: $La_{1-x}Sr_xMnO_3$. *Phys. Rev. Lett.* **75,** 109–112 (1995).
15. Hwang, H. Y., Cheong, S.-W., Ong, N. P. & Batlogg, B. Spin-polarized intergrain tunneling in $La_{2/3}Sr_{1/3}MnO_3$. *Phys. Rev. Lett.* **77,** 2041–2044 (1996).
16. de Boer, P. K., van Leuken, H., de Groot, R. A., Rojo, T. & Barberis, G. E. Electronic structure of $La_{0.5}Ca_{0.5}MnO_3$. *Solid State Commun.* **102,** 621–626 (1997).
17. Pickett, W. E. & Singh, D. J. Electronic structure and half-metallic transport in the $La_{1-x}Ca_xMnO_3$ system. *Phys. Rev. B* **53,** 1146–1160 (1996).
18. Lu, Y. *et al.* Large magnetotunneling effect at low magnetic fields in micrometer-scale epitaxial $La_{0.67}Sr_{0.33}MnO_3$ tunnel junctions. *Phys. Rev. B* **54,** R8357–R8360 (1996).
19. Sun, J. Z., Krusin-Elbaum, L., Duncombe, P. R., Gupta, A. & Laibowwitz, R. B. Spin-polarized tunneling in doped perovskite manganate trilayer junctions. *Appl. Phys. Lett.* **70,** 1769–1771 (1997).
20. Kwon, C. *et al.* Stress-induced effects in epitaxial $(La_{0.7}Sr_{0.3})MnO_3$ films. *J. Magn. Magn. Mater.* **172,** 229–236 (1997).
21. Vescovo, E. *et al. The U5UA SGM-beamline: First Tests on the Performances A-25* (Activity Rep. 1996, National Synchrotron Light Source, Brookhaven National Lab, Upton, 1997).
22. Sarma, D. D. *et al.* Temperature-dependent photoemission spectral weight in $La_{0.6}Sr_{0.4}MnO_3$. *Phys. Rev. B* **53,** 6873–6877 (1996).
23. Saitoh, T. *et al.* $La_{1-x}Sr_xMnO_3$ studied by photoemission and X-ray absorption spectroscopy. *Phys. Rev. B* **51,** 13942–13951 (1995).
24. Trajanovic, Z. *et al.* Growth of colossal magnetoresistance thin films on silicon. *Appl. Phys. Lett.* **69,** 1005–1007 (1996).

Acknowledgements. We thank J. Hastings for discussions. NSLS is supported by the US Department of Energy; the work in the University of Maryland was partially supported by the US Office of Naval Research.

Correspondence and requests for materials should be addressed to J.H.P. (e-mail: jhpark@bnlls1.nsls.bnl.gov).

A soft magnetic CoNiFe film with high saturation magnetic flux density and low coercivity

Tetsuya Osaka*, Madoka Takai*, Katsuyoshi Hayashi*, Keishi Ohashi†, Mikiko Saito‡ & Kazuhiko Yamada‡

** Department of Applied Chemistry, Waseda University, and Kagami Memorial Laboratory for Material Science and Technology, Waseda University, Shinjuku-ku, Tokyo 169, Japan*

† NEC Ibaraki Ltd, Sekijomachi, Makabegun, Ibaraki 308-01, Japan

‡ NEC Corporation, Fuchu, Tokyo 183, Japan

Magnetic materials are classed as 'soft' if they have a low coercivity (the critical field strength H_c required to flip the direction of magnetization). Soft magnetic materials are a central component of electromagnetic devices such as step motors, magnetic sensors, transformers and magnetic recording heads. Miniaturization of these devices requires materials that can develop higher saturation flux density, B_s, so that the necessary flux densities can be preserved on reducing device dimensions, while simultaneously achieving a low coercivity. Common high-B_s soft magnetic films currently in use are electroplated CoFe-based alloys[1–4], electroplated CoNiFe alloys[5–7], and sputtered Fe-based nanocrystalline[8–11] and FeN films[12–14]. Sputtering is not suitable, however, for fabricating the thick films needed in some applications, for which electrochemical methods are preferred. Here we report the electrochemical preparation of a CoNiFe film with a very high value of B_s (2.0–2.1 T) and a low coercivity. The favourable properties are achieved by avoiding the need for organic additives in the deposition process, which are typically used to reduce internal stresses. Our films also undergo very small magnetostriction, which is essential to ensure that they are not stressed when an external magnetic field is applied (or conversely, that external stresses do not disrupt the magnetic properties). Our material